THERMAL ANALYSIS OF THE INTERNAL ENVIRONMENT OF SARA SUB-ORBITAL PLATFORM

Carlos Lavrado Filho, eng.lavrado@gmail.com
Faculdade de Engenharia, Arquitetura e Urbanismo – FEAU
Universidade do Vale do Paraíba – UNIVAP
Av. Shishima Hifume, 2911, Urbanova, 12244-000
São José dos Campos, SP

Humberto Araujo Machado, humbertoam@iae.cta.br
Instituto de Aeronáutica e Espaço – IAE
Comando-Geral de Tecnologia Aeroespacial – CTA
Pr. Mal. Eduardo Gomes, 50, Vila das Acácias, 12228-904
São José dos Campos, SP

Faculdade de Tecnologia – FAT
Universidade do Estado do Rio de Janeiro – UERJ
Rodovia Presidente Dutra, km 298 RJ-SP
Resende, RJ

Abstract. *Sub-orbital platforms are a low-cost alternative for micro-gravity research. The internal environment of such platform should be carefully controlled in order to assure the correct temperature for the experiments being performed. In this work the thermal behavior of the internal environment of the sub-orbital SARA platform is studied in all phases of the mission. The maximum temperature reached is calculated via an integral analysis. It is observed that the major external heat source is the solar radiation during the pre-flight period, and its effect can be greatly reduced through the use of the decorative ink already used in the rocket engine surface. The differential analysis of the shipped electronic equipment shows the existence of two critical points in the circuits. However, this result was obtained considering that the fully electrical power was transformed in heat, what should be revised employing more realistic values.*

***Keywords**: Sub-orbital platform, Thermal analysis, Internal environment.*

1. INTRODUCTION

Sub-orbital platforms are a low-cost alternative for micro-gravity research. The SARA sub-orbital platform is being developed by IAE/CTA for this application, Fig. 1. Its total mass is 250 kg for a payload of about 25 kg. The sub-orbital version is designed to provide 6 minutes of micro-gravity environment. In the future, the orbital version is expected to reach an orbit of 300 km around the Earth during 10 days (Moraes, 1998)

The platform is equipped with an external thermal shield for protection against aerodynamic heating due the very high velocities reached at itsascent flight and reentry. Although this shield assures protection against the external heating, there is no active system of refrigeration inside the sub-orbital version, to control the temperature in the internal environment. This environment should be carefully controlled to assure the correct temperature for the experiments assembled. In order to keep the internal temperature under control, all heat sources have to be taken into account, and also the external ones, like the solar radiation and the fraction of external aerodynamic heat that crosses the wall. This estimation may include all periods of the mission, including the pre-launching phase, when the platform stays at the launchpad. In this work the thermal behavior of the internal environment of the sub-orbital SARA platform is studied, in all phases of the mission. A combination of integral and differential analysis is done, in order to estimate the maximum temperatures reached inside SARA.

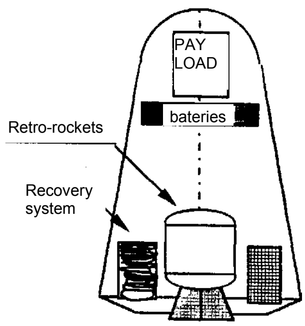

Figure 1. SARA sub-orbital platform and its internal systems.

2. PHYSICAL PROBLEM

2.1. Physical characteristics of SARA

For an integral analysis the partitions and internal systems of the platform, as described by Da Costa et al. (2007), can be grouped and considered as homegeneous regions, with constant properties and temperatures, as represented in Fig. 2. Dimensions, materials and properties of each region are showed in Tabs. 1-3. The temperature limit for the internal environment was fixed in 60^o C. The maximum time for standing at launchpad is two hours, until 11:00 am.

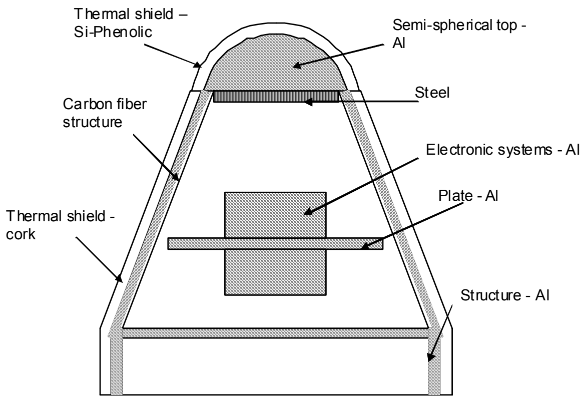

Figure 2. Partition assumed for SARA.

Table 1. Main dimension of SARA sections (Machado, 2006).

Section	**External surface (m^2)**	**Internal volume occupied by air (m^3)**
Semi-spherical top	0.3488	Solid
Cone	3.08	0.6215
Cylindrical basis	1.081	Opened

Table 2. Physical properties of materials employed (Machado. 2006).

Property\ Material	**Steel**	**Aluminum**	**Carbon fiber**	**Si-Phenolic**	**Cork**
Emissivity	0.11	0.06	1	0.8	0.78
Specific heat (J/kg K)	500	960	800	1256	1971.8
Thermal conductivity (W/m K)	16.2	177	150	0.485	0.084
Density (kg/m^3)	8000	2710	1750	1730	480
Ablation temperature (^{o}C)	-	-	-	538	260

Table 3. Material and mass of each partition (Da Costa et al.. 2007).

Partition	**Material**	**Mass (kg)**
Structure (conic section)	Carbon fiber	21.0084
Superior plate	Stainless steel	6.6616
Middle plate	Aluminum	151.8783
Closing plate	Aluminum	
Structure (cylindrical section)	Aluminum	
Electronic systems	Aluminum	
Semi-spherical top	Aluminum	
Top thermal shield	Si-Phenolic	16.4626
Lateral thermal shield	Cork	3.3303

2.2. Heat transfer processes

Figure 3 shows the heat transfer processes that happen in SARA. Some occurs simultaneously. Some are present in specific periods of the mission. Next, each process is described and mathematically modeled.

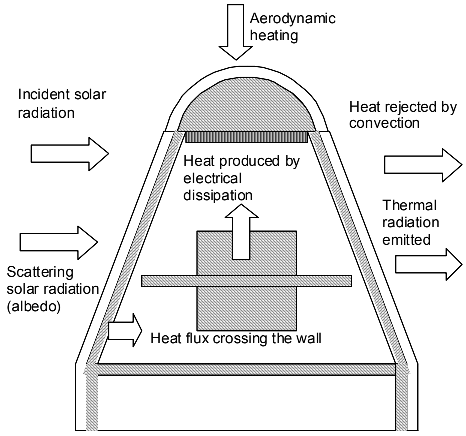

Figure 3. Heat transfer processes during a mission.

Aerodynamic heating: due the convection between the surface and the air at high temperatures, when the platform reaches hypersonic velocities. Machado (2006) has previously studied this process, and demonstrated that the thermal shield keeps the temperature bellow 50^o C. In order to have a conservative result, it will be considered that the internal temperature of the wall reaches the maximum value allowed, 60^o C, as a consequence of this external heating.

External convection at launchpad: here the heat Exchange between SARA external surface and environment during the pre-flight period is estimated. The most critical situation is natural convection (absence of wind), with a film coefficient h_{oo} = 6 W/m^2.^{o}C (Kreith and Bohn, 2003) and an environment temperature T_{oo} = 300 K (27^o C). The heat flux is:

$$q_{cn} = h_\infty (T_w - T_\infty) \tag{1}$$

Incident solar radiation: is the solar radiation that straight impacts the external surface, varying with the daytime, Fig. 4. It is considered function of time, and interpolated by a fourth degree polynomial in the interval between 9:00 am and 11:00 am (time interval reserved for the launching). Supposing the external surface acts as black body, absorvity is considered equal to emissivity. The heat flux will be:

$$q_{sd} = \alpha . f(t) \tag{2}$$

where α us the absorvity of wall external surface, t is the time and $f(t)$ is the interpolation polynomial.

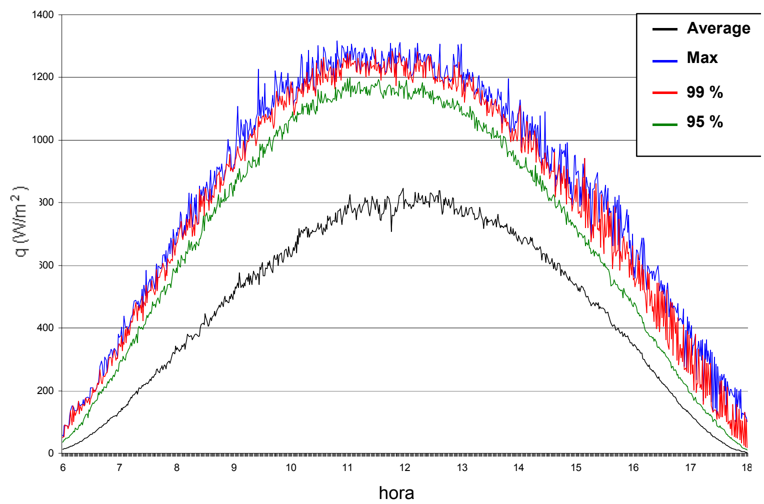

Figure 4. Solar radiation during day light measured at CLA (*Centro de Lançamento de Alcântara*) (Fisch, 2005).

Albedo: is the solar radiation scattered by the environment, reaching the external surface. The *albedo* (η) allows estimating this term as fraction of the incident solar radiation:

$$q_{si} = \eta . q_{sd} \tag{3}$$

where $\eta = 0,3$ in CLA, obtained from *in situ* measurements (Fisch, 2005).

Thermal radiation emitted by the external wall: is the heat rejected by the wall as thermal radiation:

$$q_{re} = \varepsilon\sigma(T_w^4 - T_\infty^4) \tag{4}$$

where ε is the emissivity of the external wall and σ is the Boltzmann constant, equal to 5,67 x 10^{-8} W/m^2K^4.

Heat flux through the wall: the heat flux that crosses the wall may be estimated via the Fourier Law:

$$q_{cond} = -k\left.\frac{\partial T}{\partial n}\right|_{parede} \tag{5}$$

Heat generation by electrical dissipation: is the heat dissipated by the electronic equipment assembled inside the platform. Since there is no information about thermal or electric efficiency of such equipment, the whole electric power will be considered:

$$\dot{W} = \sum U_i . A_i \tag{6}$$

where $\dot{W}$ is the total power dissipated, U_i is the voltage and A_i is the electrical current in each device.

3. MATHEMATICAL MODELING AND ANALYSIS

3.1. Heat transfer in the wall

The transient response of the wall concerned to the heat exchange with the external environment should be verified. Machado (2006) has already done such analysis for the flight period, resulting in a low rising of internal temperature, as mentioned. For the pre-flight period, it will be considered one-dimensional transient conduction through the wall in the major surface, i.e., the conic region made by carbon fiber and covered with cork. The energy balance is shown in Fig. 5, and results in Eq. (7).

$$q_{cond} = q_{sd} + q_{si} - q_{cn} - q_{re} \tag{7}$$

Expanding all terms, according to Eqs.(1-5)::

$$-k\left.\frac{\partial T}{\partial x}\right|_{x=0} = \alpha f(t) + \eta\alpha f(t) - h_\infty(T_w - T_\infty) - \varepsilon\sigma(T_w^4 - T_\infty^4) \tag{8}$$

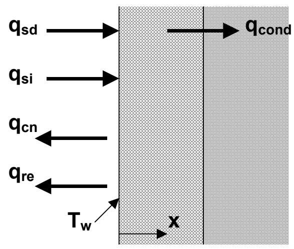

Figure 5. Energy balance in the wall.

If the internal side of the wall is assumed to be thermally insulated, when the system reaches steady state the wall heat flux should be zero, and the derivative in the left side of Eq. (8) will be zero. The emissivity of the external side is assumed to be equal to the cork emissivity, and to behave as a black body, $\alpha = \varepsilon$. Taking a constant value for *f(t)*, equal to 1.134,95 W/m^2 (average of the polynomial between 9:00 am and 11:00 am), a wall temperature of 113.7° C is obtained for steady state. The time spent for the cork to reach steady state may be determined through an integral analysis, considering the whole cork layer temperature equal to the surface temperature:

$$mc_p \frac{dT}{dt} = A\left[\alpha f(t) + \eta \alpha f(t) - h_\infty (T_w - T_\infty) - \varepsilon\sigma (T_w^4 - T_\infty^4)\right] \tag{9}$$

where m and c_p are the mass and specific heat of cork layer, respectively, and A is its area, all the values extracted from Tabs. 1-3. Equation (9) is solved numerically by a single time marching integration, and the steady state is reached after about 10 minutes. Since the minimum time exposition of the platform in the pre-flight period is two hours, in all cases the structure will be considered perfectly permeable to the heat, and the time for heat diffusion will be neglected.

3.2. Integral analysis of the pre-flight period

From the previuos results and hypothesis assumed in the previous section, the balance of energy in SARA will be done considering a homegeneous temperature in the whole platform:

$$C\frac{dT}{dt} = A\left[af(t) + \eta af(t) - h_\infty (T_w - T_\infty) - \varepsilon\sigma (T_w^4 - T_\infty^4)\right] + \dot{W} \tag{10}$$

where C is the total heat capacity of SARA, obtained from:

$$C = \sum m_i c_{p_i} \tag{11}$$

where m_i and c_{pi} are the mass and specific heat of each partition. Beyond the material listed in Tab.3, the air inside SARA should also be added to the calculation. The air mass is obtained from the application of the ideal gas law for the internal platform volume, Tab. 1, resulting in a mass of 0.7314 kg, with a c_p = 1004 J/kg.K. The result for C is 194 kJ/K. For an initial temperature of 300 K, the solution of Eq.(10) results in a steady state temperature of 116.5° C. For two hours of exposition, SARA mean temperature reaches 109.4°C, that surpass the temperature limit of 60° C.

This result showed that a thermal protection is needed for the external surface during the pre-flight time. The option is the decorative ink already used in some space vehicles developed by IAE/CTA, with reflective and insulation properties (Lavrado Filho and Machado, 2007). According to Garcia (1996), ink's absorvity in the solar band is $\alpha = 0.164$ and the emissivity in the infrared band is $\varepsilon = 0.898$. The solution of Eq.(10) is now obtained with these new values, for the constant average value of the incident solar radiation and considering its variation with time, Fig. 6. In the first case, Fig. 6.a, after two hours of exposition the steady state temperature falls to less than 50° C. In the second case, Fig. 6.b, the temperature peak is reached at approximately 10:00 am, and falls continuously from that instant. Therefore, painting the external surface of SARA with this decorative ink is enough to warrant that the temperature is kept bellow the limit during the pre-flight period.

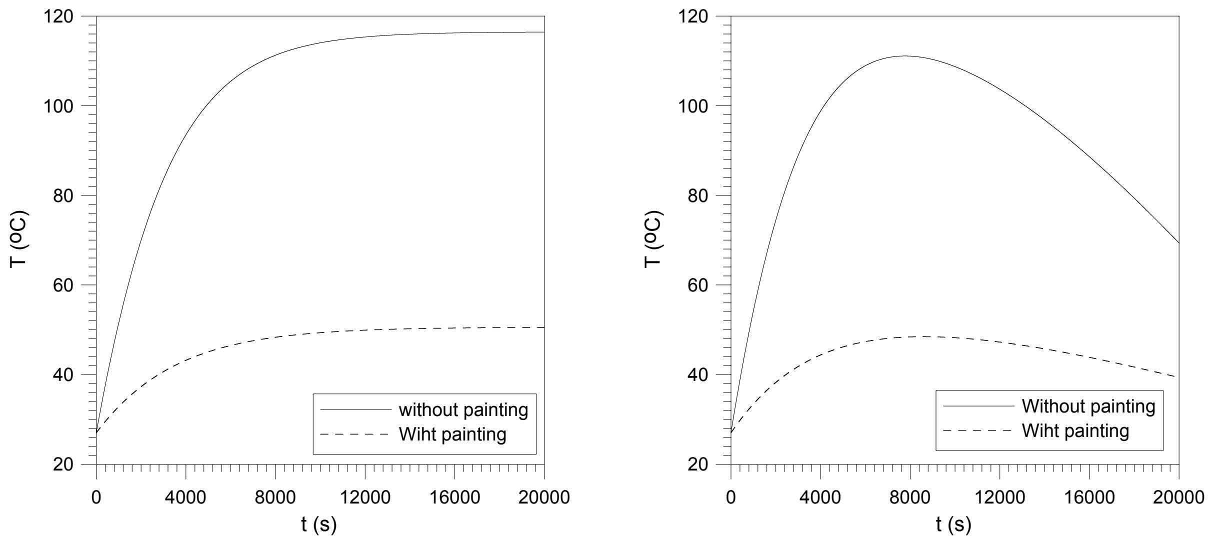

(a) Average valor for solar radiation *(b) Solar radiation as a function of time*

Figure 6. Numerical solution of Eq.(10).

Once the problem of external heating by solar radiation has been solved, the only heat source acting over the internal environment will be the thermal dissipation of the electronic equipment. Considering the internal surface thermally insulated, an estimative is done by taking into account the presence of the air and electronic devices. In this case, Eq. (10) is modified:

$$C_{se}\frac{dT}{dt} = A\left[-h_{ai}(T_w - T_{ai})\right] + \dot{W} \tag{12}$$

where C_{se} is the heat capacity of electronic systems, h_{ai} is the film coefficient for internal convection, assumed to be 6 W/m^2.K and T_{ai} is the temperature of the air inside, obtained from:

$$C_{ai}\frac{dT_{ai}}{dt} = A\left[h_{ai}(T_w - T_{ai})\right] \tag{13}$$

Replacing Eq.(13) in Eq.(12):

$$C_{se}\frac{dT}{dt} = \dot{W} + C_{ai}\frac{dT_{ai}}{dt} \tag{14}$$

The solution of Eq.(14) for C_{se} = 103.65 kJ/K e C_{ai} = 734.3 J/K yields a maximum value of 41.2^{o}C, that is bellow the temperature limit. It should be noted that the temperature increases linearly with time, at a rate of 7,1^{o}C/h, what should be considered for major periods of exposition.

3.3. Internal heating during flight

For this period, it will be considered the worst situation, i.e., internal wall temperature reaches the limit (60^o C) quickly, and keeps in this value during the whole trajectory, with duration of 725 s. Eq.(12) is applied for constant air temperature of 60^o C. The surface for heat exchange was considered equal to the surface of the conic section. This is a conservative approach, since the actual surface for heat exchange of the electronic systems should be smaller, because they are inside this partition. The maximum temperature reached was 44.8^o C, starting from the value found in the end of the pre-flight period (41.2^o C), with a constant rate of warming of 0.1^o C/min.

3.4. Critical points

Once the integral analysis showed that the mean internal temperature do not surpass the limit, the electronic equipment have to be analyzed separately, in order to verify the presence of critical points of heating. The power data for each electronic device was extracted from the manufacturer's specification (Carvalho, 2006). Due to the lack of detailed information about each particular component, the physical properties used were that of the Al, except the mean specific mass, obtained from the design specification (Da Costa et al., 2007), divided by its volume. As mentioned, the dissipation is considered to be the full electric power (electric current x voltage) in each component of the electronic system.

For calculation, the electronic systems, the plates (internal and closing ones) and the system base structure were taken as the domain of simulation. All the surfaces were assumed to be exposed to natural convection with the internal air that is kept at 27^o C. The value for the film coefficient employed was 6 W/m^2.^{o}C.

The computational simulation of heat conduction in the electronic equipment was done via the Finite Element method, through the software COSMOS (Dassault Systemes S.A., 2004). In Fig. 7 the component distribution and the mesh over the domain is showed. In some point the geometry was simplified, in order to allow the full discretization of the domain.

Figure 8 shows the final temperature distribution after two hours. In the major part of the domain, the temperature keeps bellow the limit. Only in two specific components (transponders and DDT's), temperature highly surpass the limit, reaching more than 160^o C, because of the high power of these components, its small volume and proximity to other heat sources. However, such results should be considered conservative, since in the actual situation, not all power supply is transformed in heat. If such temperature levels are confirmed, an active refrigeration system will be necessary.

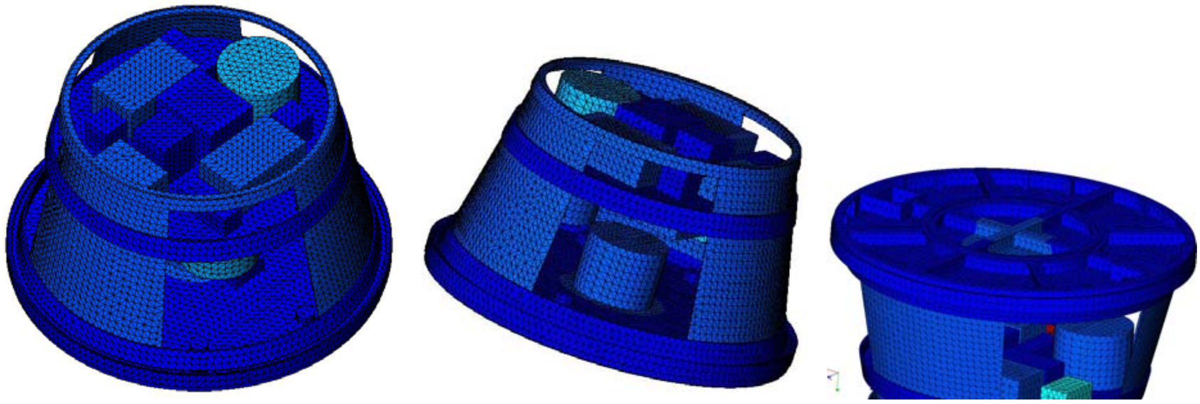

Figure 7. Mesh used in the simulation.

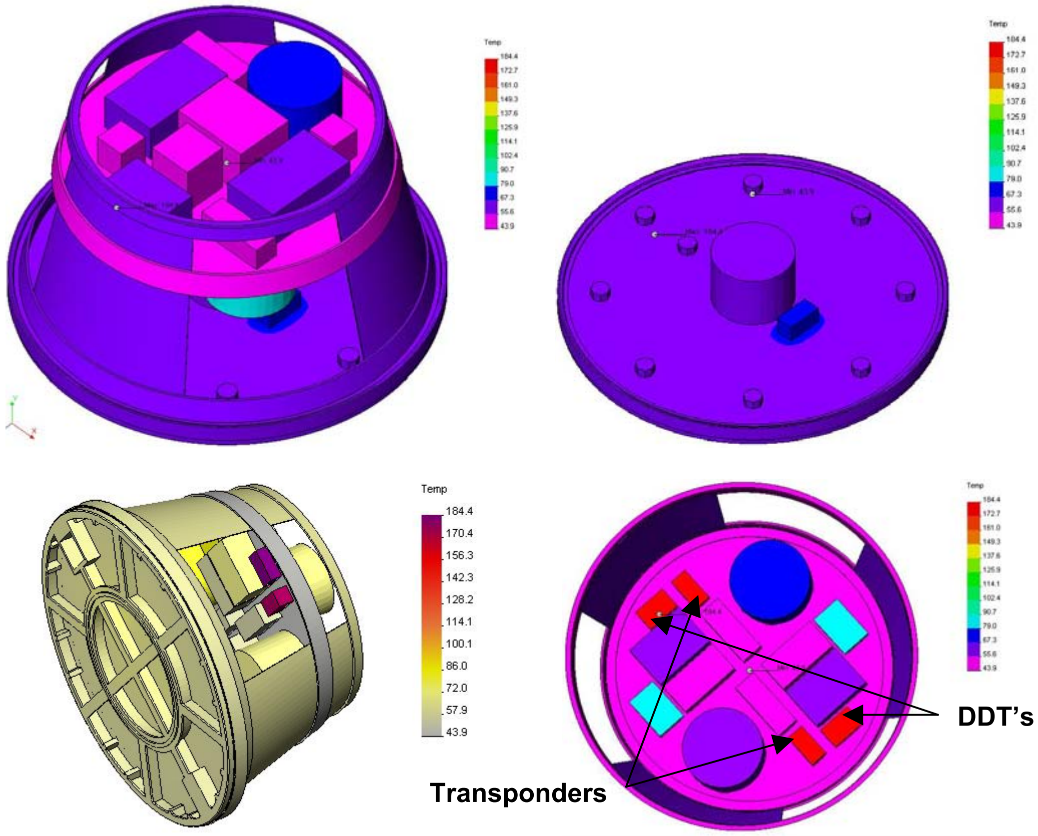

Figure 8. Temperature distribution inside SARA after two hours.

4. CONCLUSION

In this work the thermal behavior of internal environment of the SARA sub-orbital platform was studied. The periods of flight and pre-flight were analyzed using integral and differential approaches. The simulation of heat exchange between the platform and the external environment showed that a thermal protection in the external surface is necessary against the solar radiation, otherwise the internal temperature may surpass the upper limit. Painting the external surface with a decorative ink solves this problem, keeping the internal temperature bellow the limit.

The differential analysis of the heating by electric dissipation presented two critical points where the temperature highly surpasses the limit. However, since the heat generation by the electronic devices was considered equal to the power supply, this surely is a conservative result. Actual values of heat dissipation obtained for each device should be used in the simulation, for a more trustable result.

The simple method used in this work can be applied for a preliminary analysis in all vehicle during its development, what can save time when compared with more detailed analysis.

5. REFERENCES

Carvalho, C. A. de P., 2006, "Redefinição das Redes Elétricas do VS-40/SARA Suborbital", Technical Report RE06006A (28/10/2006), Mectron, são José dos Campos.

Da Costa, L. E. V. L., Silva F. de A. and De Souza, C. E., 2007, "SARA Suborbital: Configuração Básica", Technical Report 717-000000/A4001, IAE/CTA, São Jose dos Campos (26 de março).

Dassault Systemes S.A., 2004, "Cosmos User's Guide".

Fisch, G., 2005, "Incidência de Radiação Solar no CLA", Internal Communication - ACA, IAE/CTA, São José dos Campos.

Garcia, E. C., 1996, "Medidas de Propriedades Termo-Ópticas", Doc. LIT.PG 004/96, INPE, São José dos Campos.

Kreith, F. and Bohn, M. S., 2003, "Princípios de Transferência de Calor", Thomson Learning, São Paulo.

Lavrado Filho, C. and Machado, H.A. 2007, "Effect of Solar Heating over the Propellant Temperature in a Solid Rocket Engine", COBEM 2007, Brasília.

Machado, H.A., 2006, "Proteção térmica para Aquecimento Aerodinâmico da Plataforma Sub-orbital SARA", CONEM 2006, Recife.

Moraes Jr., P., 1998, "Design Aspects of the Recoverable Orbital Platform SARA", Proceedings of 8th Chilean Congress of Mechanical Engineering, Concepcíon, Chile.

6. RESPONSIBILITY NOTICE

The authors are the only responsible for the printed material included in this paper.